Spatial Evolution of the Ferromagnetic Phase Transition in an Exchange Graded Film

B. J. Kirby,[1,*] H. F. Belliveau,[2] D. D. Belyea,[2] P. A. Kienzle,[1] A. J. Grutter,[1] P. Riego,[3] A. Berger,[3,†] and Casey W. Miller[4,‡]
[1]*Center for Neutron Research, NIST, Gaithersburg, Maryland 20899, USA*
[2]*Department of Physics, University of South Florida, Tampa, Florida 33620, USA*
[3]*CIC nanoGUNE Consolider, E-20018 Donostia–San Sebastian, Spain*
[4]*School of Chemistry and Materials Science, Rochester Institute of Technology, Rochester, New York 14623, USA*
(Received 4 May 2015; published 29 January 2016)

A combination of experiments and numerical modeling was used to study the spatial evolution of the ferromagnetic phase transition in a thin film engineered to have a smooth gradient in exchange strength. Mean-field simulations predict, and experiments confirm, that a 100 nm Ni_xCu_{1-x} alloy film with Ni concentration that varies by 9% as a function of depth behaves predominantly as if composed of a continuum of uncoupled ferromagnetic layers with continuously varying Curie temperatures. A mobile boundary separating ordered and disordered regions emerges as the temperature is increased. We demonstrate continuous control of the boundary position with temperature, and reversible control of the magnetization on both sides of the boundary with the magnetic field.

DOI: 10.1103/PhysRevLett.116.047203

Precise fabrication of magnetic heterostructures can lead to the control of physical properties, including magnetic ordering. Ramos *et al.* [1], for example, showed that heterostructures composed of antiferromagnetic materials with nominally independent order parameters can exhibit a single phase transition at intermediate temperatures; Wang and Mills provided a mean-field theoretical treatment for such systems [2]. Similarly, Marcellini *et al.* used finite size effects to study the novel magnetic ordering of Fe/V multilayers in which each layer had distinct ordering temperatures [3]. Complementing these traditional heterostructures, recent work has explored materials with novel functionality derived from smoothly changing the films' physical properties during growth. Examples applicable to next generation magnetic recording involved graded magnetic anisotropy [4–8] and the recent demonstration of a movable antiferromagnet-ferromagnet phase boundary in doped FeRh films [9].

This Letter considers a ferromagnetic thin film with exchange strength J that varies continuously through its thickness. Within the mean-field approximation (MFA), J is proportional to the Curie temperature T_C, meaning that a structure composed of distributions of J can be thought of as having a distribution of "local" Curie temperatures T_C'. From a thermodynamics viewpoint, an exchange coupled multilayer is considered to have a single "global" Curie temperature, corresponding to long-range order throughout the structure [2,10]. However, the degree to which exchange coupling impacts depth-dependent properties in real materials has not been thoroughly studied. To explore the case of an exchange strength gradient, we chose nickel-copper alloy as a model system, because it forms isomorphous solid solutions, and it exhibits T_C that changes linearly with composition [11,12]. By varying the nickel content during growth, a rational distribution of J (and thus T_C') can be achieved in films with well-controlled depth (z) dependent composition, e.g., $Ni_{x(z)}Cu_{1-x(z)}$.

100 nm thick (111) textured $Ni_{x(z)}Cu_{1-x(z)}$ alloy films capped with 5 nm Ta were deposited on Si substrates using room temperature sputtering. Composition gradients were achieved by adjusting the deposition rates from two independent magnetron guns. Computer control allowed the net deposition rate to remain constant throughout codeposition. The graded sample composition varied linearly from $x = 0.61$ near the substrate to 0.70 at the top of the film. Uniform control samples with $x = 0.61$ and $x = 0.70$ were also grown. Figure 1 shows the derivative

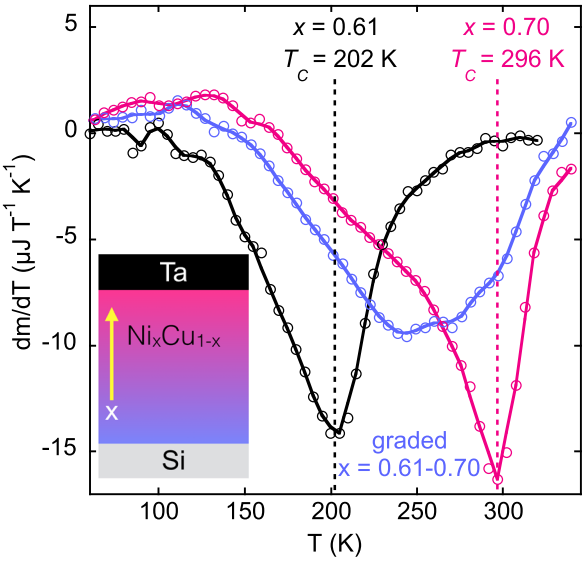

FIG. 1. Derivative of magnetic moment with respect to temperature for the uniform $x = 0.61$ (black), graded $x = 0.61$–0.70 (purple), and uniform $x = 0.70$ (pink) samples.

of the magnetic moment with respect to temperature (T) for the samples, as measured in a 60 mT in-plane field with vibrating sample magnetometry. The T-dependent derivatives for the uniform samples exhibit distinct minima at 202 and 296 K, indicative of their respective T_C. The corresponding peak for the graded sample falls in between, but is significantly broader. This suggests that the magnetic ordering takes place over a wide range of temperatures, as the ferromagnetically ordered fraction of the film shrinks in volume with increasing temperature.

The temperature- and field-dependent depth profile was treated theoretically via an exchange strength gradient model (ESG), which was solved numerically in MFA [13,14]. 500 layers of ferromagnetically coupled spins were arranged on a fcc(111) lattice with 0.2 nm lattice spacing, magnetic moment in the (111) plane, and depth-dependent J. Given the translational invariance within the plane of each layer i, the spin variables in i result in one thermodynamic average for the magnetization m_i only, a fact that implicitly introduces a quasi-infinite interaction range within each plane via the MFA. This is in contrast to other methodologies, e.g., nearest-neighbor Monte Carlo simulations [15]. However, the translational invaraiance is broken along the z axis perpendicular to the (111) planes to account for the expected gradient in J, and thus T'_C [Fig. 2(a)]. It is important to note that the interlayer exchange coupling in the simulation is strong: half of the total exchange field originates from interlayer coupling for the fcc(111) lattice.

Figure 2 shows the results of simulations in both zero ($h = 0.00$) and nonzero ($h = 0.01$) applied field for different temperatures. The applied magnetic field h is given as a fraction of the exchange field at the high x end of the sample $6J(x = 0.71)S$ at $T = 0$ K, and is thus unitless. m is also unitless, normalized by the depth-independent saturation magnetization. When the temperature exceeds some of the T'_C values with $h = 0.00$ [Fig. 2(b), lower curve], the layer divides into strongly and weakly (effectively zero) ordered regions. The quasiphase boundary [16] separating these regions, which we call the "Curie depth," z_C, corresponds directly to the location with T'_C equaling the sample temperature. Once the applied field is increased to $h = 0.01$ [upper curve, Fig. 2(b)], the magnetization increases everywhere, particularly so near z_C. As such, the boundary at z_C can be thought of as separating a strongly ferromagnetic region from a region that exhibits paramagnetic character. Figure 2(c) shows that z_C increases significantly as T increases from 0.84 to 0.91, moving closer to the high T'_C end of the structure. Thus, the simulation predicts a boundary between weakly and strongly ordered regions that can be moved continuously along the growth axis with temperature, and that the magnetization on both sides of that boundary can be controlled with applied field. Notably, both of these functionalities are reversible, as this is a second-order phase transition without metastable states.

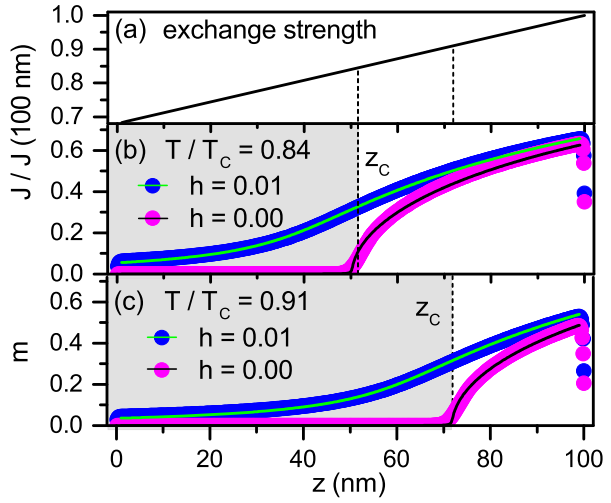

FIG. 2. Exchange strength gradient model. (a) Depth-dependent exchange strength. (b), (c) Magnetization profiles at 0.84 T_C and 0.91 T_C, respectively. Symbols in (b) and (c) are the results of mean-field simulations, solid curves are fits using a closed-form function. Dashed vertical lines in (b) and (c) indicate z_C.

Despite the inherently strong interlayer coupling in our model system, our numerical results appear to be very similar to what one would expect from magnetically decoupled layers with distinct T_C. To investigate and eventually utilize this fact for our data analysis, we calculated the expected magnetization profiles for such uncoupled layer systems. In MFA, for a layer i of $S = \frac{1}{2}$ spins with uniform exchange coupling strength J and thus one specific local Curie temperature T'_{Ci}, the self-consistency equation to determine its temperature-dependent magnetization m_i is given by

$$m_i(T) = \tanh\left[\frac{T'_{Ci}}{T}[m_i(T) + h]\right]. \quad (1)$$

Dropping the subscript i and defining the local Curie temperature as $T'_C(z) = T + a(z - z_C)$, Eq. (1) can be solved formally as

$$z = z_C + \frac{1}{A}\left[\frac{\tanh^{-1}(m)}{m + h} - 1\right], \quad (2)$$

where $A = a/T$ is the temperature normalized T'_C gradient in units of inverse length. The $z(m)$ function can be transformed into a closed-form $m(z)$ expression using a series expansion of $\tanh(x)$ up to third order in x [17]. This $m(z)$ function was fitted to the simulation data of the exchange gradient model using z_C and h as free parameters and is shown as solid curves in Figs. 2(b) and 2(c). The agreement between the full simulation and the local T'_C calculation is excellent, with the fitted values of h matching the simulation inputs. Deviations only occur for vanishing h, and only within about 1 nm of z_C. This consistency

suggests that interlayer exchange coupling does not lead to a large spatial spread of the phase transition in exchange graded films, and that the predominant temperature and field evolution of such films can be given by a continuum of J or T_C'. This is consistent with earlier results on three-dimensional multiphase nanostructures, for which a coupling or penetration length of only a few interatomic distances was found [10].

To experimentally probe the nature of the ferromagnetic phase transition, polarized neutron reflectometry (PNR) was used to determine the temperature and applied magnetic field (H) dependent magnetization depth profiles of the $Ni_{x(z)}Cu_{1-x(z)}$ sample. Measurements were taken over a range of temperatures with in-plane fields of either 5 or 500 mT using the PBR beam line at the NIST Center for Neutron Research [18–21]. For a PNR measurement [22], model fittings of R^{++} (incident and scattered neutron moment parallel to H) and R^{--} (incident and scattered antiparallel) are used to determine the depth profiles of the nuclear scattering length density ρ_N and the component of the sample magnetization (M) parallel to H.

PNR data measured in 500 mT at 145 and 293 K are shown in Fig. 3(a). The clear spin-dependent oscillations demonstrate sensitivity to the nuclear and magnetic depth profiles. To highlight the magnetic contribution to the scattering, the data in Fig. 3(a) are plotted in Figs. 3(b) and 3(c) as spin asymmetry (the difference in R^{++} and R^{--} divided by the sum). The amplitude of the spin asymmetry drops appreciably with increased T, corresponding to the drop in magnetization.

At low T, the data can be fitted reasonably well by a model featuring a linear gradient in M, or even a NiCu layer of uniform composition and magnetization. However, these models become progressively less effective as T is increased [22–25]. On the contrary, the 500 mT data at all T are fit extremely well by the ESG model outlined above. Specifically, the magnetic profiles are based on the closed-form $m(z)$, convoluted with a sloped line to account for the expected variation in total magnetic moment, and multiplied by the saturation magnetization (M_S) of the high x end,

$$M(z) = M_S\left(\frac{1-\frac{x_i}{x_f}}{t}z + \frac{x_i}{x_f}\right)m(z), \tag{3}$$

where t is the total thickness of the $Ni_{x(z)}Cu_{1-x(z)}$ layer, $x_i = 0.61$, and $x_f = 0.70$. We assume a linear distribution

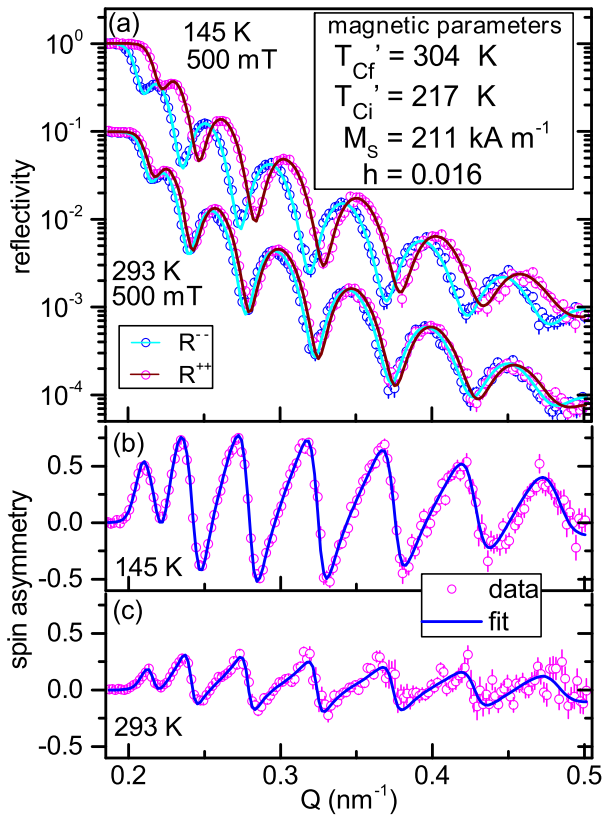

FIG. 3. (a) Fitted PNR data. Inset shows best-fit magnetic parameters. 2σ fitting uncertainties are < 3 K for T_{Ci} and T_{Cf}, < 2 kA m^{-1} for M_S, and < 0.002 for h. (b),(c) Fitted data in (a) plotted as spin asymmetry. Error bars correspond to $\pm 1\sigma$.

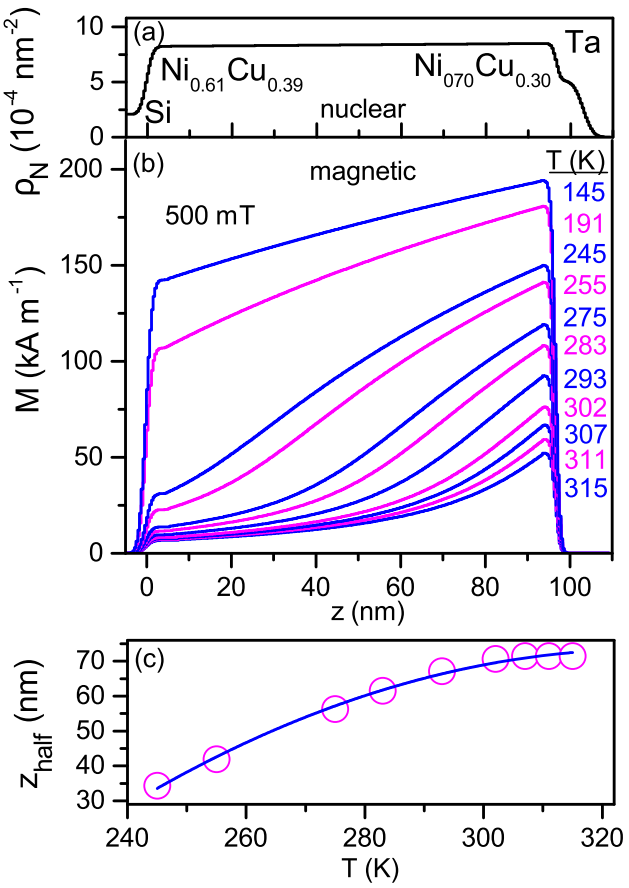

FIG. 4. Nuclear (a) and magnetic (b) profiles corresponding to the fits in Fig. 3. (c) Temperature dependence of the depth corresponding to half the maximum magnetization. Solid curve is a guide to the eye.

of T'_C, such that the T-dependent Curie depth can be described in terms of the top (f) and bottom (i) T'_C:

$$z_C(T) = \frac{T - T'_{Cf}}{T'_{Cf} - T'_{Ci}} t. \quad (4)$$

Data measured at all conditions (including 5 mT data discussed below) were simultaneously fit using a consistent model with only five magnetic parameters: T'_{Cf}, T'_{Ci}, M_S, h(500 mT), and h(5 mT). The fits are excellent, with examples shown as solid curves in Fig. 3, associated magnetic fitting parameters shown in the Fig. 3(a) inset, and the corresponding profiles shown in Figs. 4(a) and 4(b). The bottom and top values of T'_C are 217 and 304 K, with 2σ fitting uncertainty less than ± 3 K. Notably, this difference in T'_C is very similar to the difference in T_C estimated for the uniform boundary condition samples. This z-dependent T'_C is manifested in the Fig. 4(b) magnetic profiles. At 145 K (well below T_C of $x = 0.61$ boundary condition sample), the entire $Ni_{x(z)}Cu_{1-x(z)}$ layer is strongly ordered. But as T exceeds 200 K, the depth profile becomes progressively more asymmetric, separating into weakly and strongly magnetized regions, with a boundary that moves continuously with T. As z_C is less obvious in high field, this moving boundary is highlighted in Fig. 4(c) in terms of z_{half}, the depth where the magnetization drops to half the maximum value. Below 240 K, this condition does not exist anywhere in the $Ni_{x(z)}Cu_{1-x(z)}$ layer, but from 240 to 302 K z_{half} moves monotonically towards the high x end before leveling off as T exceeds T'_{Cf}.

The ESG model also predicts interesting field-dependent behavior that is confirmed by the PNR data. At 275 K, H was cycled between 5 and 500 mT multiple times, with PNR measurements performed at each step. The amplitude of the spin asymmetry [Figs. 5(a) and 5(b)] drops for low fields, indicating a change in magnetic profile. The fits to the data are again quite good, with the two field conditions differing by only one fitting parameter, h, which drops from 0.016 to 0.003 (2σ uncertainty less than 0.002). While this is in good qualitative agreement with the change in H, the quantitative discrepancy is suggestive of the limits associated with our relatively simple modeling scheme. The field-dependent profiles are displayed in Fig. 5(c). At 5 mT, the sample is strongly magnetized near the top, with a magnetization near zero at the bottom. Increasing the field to 500 mT appreciably magnetizes the region near the bottom, thereby effectively increasing the magnetized thickness of the film. These data are cycle independent, meaning that these changes in magnetization are reversible with applied field.

This work shows that a smoothly graded 100 nm $Ni_{x(z)}Cu_{1-x(z)}$ alloy film exhibits a ferromagnetic phase transition similar to what one would expect from a continuum of uncoupled ferromagnetic layers with distinct Curie temperatures. Interestingly, interlayer exchange coupling plays a very minor role in the spatial evolution of the transition at length scales greater than 1 nm. This is particularly surprising because temperature-dependent exchange coupling can in some cases be strong enough to fully reverse ferromagnets [26]. As such, we demonstrate continuous control of the displacement of a quasiphase boundary between weakly and strongly magnetically ordered regions in a thin film, with field control of the magnetization on both sides of the boundary. These functionalities were designed to be most active near room temperature, but the physics applies to any temperature range that may be desired. The extension to magnetic systems with technological relevance, such as FePt, is obvious. Since the exchange length in these high anisotropy systems is only a few nm, it should be possible to engineer thin FePt films that exhibit similar behavior dictated by gradients in composition [27]. Further, since the volume of ferromagnetically ordered spins changes with temperature in these structures, one can envision novel application in thermomagnetic sensors and switches [12]. For instance, a symmetrically graded structure with the paramagnetic region in the center could show complex temperature-dependent magnetic coupling, since the thickness of the paramagnetic interlayer region will be temperature dependent. In addition, rationally designed

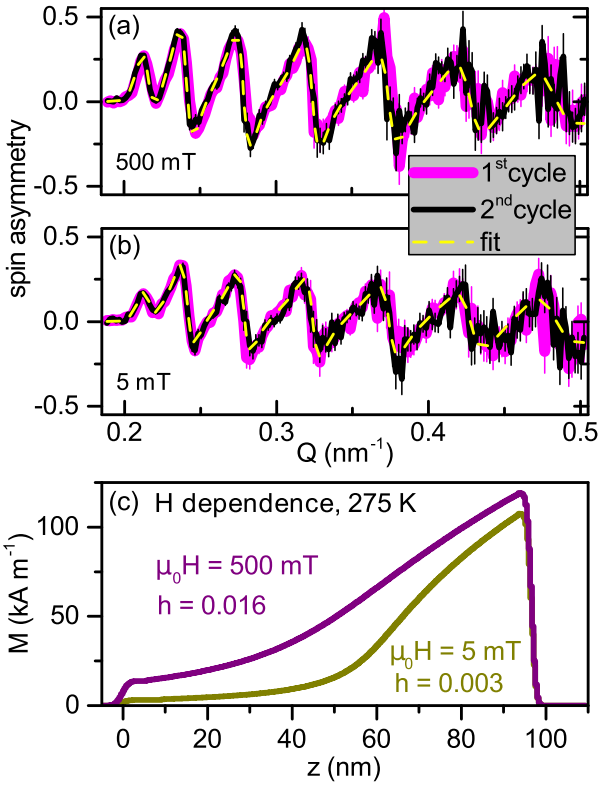

FIG. 5. (a), (b) Fitted PNR data plotted as spin asymmetry show clear reversible behavior, as well as a strong field-dependent amplitude. Error bars correspond to $\pm 1\sigma$. (c) Magnetic profiles corresponding to the fits in (a) and (b).

composition profiles could be employed to achieve specifically desired temperature and field dependencies. Such an approach could be used to tailor the magnetocaloric response of a medium to realize advances in applications such as magnetic refrigeration [28,29].

Work at RIT was supported by NSF-CAREER No. 1522927. Work at nanoGUNE was supported by the Spanish Ministry of Economy and Competitiveness through Grant No. MAT2012-36844.

*bkirby@nist.gov
†a.berger@nanogune.eu
‡cwmsch@rit.edu

[1] C. A. Ramos, D. Lederman, A. R. King, and V. Jaccarino, Phys. Rev. Lett. **65**, 2913 (1990).
[2] R. W. Wang and D. L. Mills, Phys. Rev. B **46**, 11681 (1992).
[3] M. Marcellini, M. Parnaste, B. Hjorvarsson, and M. Wolff, Phys. Rev. B **79**, 144426 (2009).
[4] D. Suess, Appl. Phys. Lett. **89**, 113105 (2006).
[5] A. Berger, N. Supper, Y. Ikeda, B. Lengsfield, A. Moser, and E. E. Fullerton, Appl. Phys. Lett. **93**, 122502 (2008).
[6] A. Berger, E. E. Fullerton, H. V. Do, and N. Supper, U.S. Patent No. 7,687,157, March 30 (2010).
[7] B. J. Kirby, J. E. Davies, K. Liu, S. M. Watson, G. T. Zimanyi, R. D. Shull, P. A. Kienzle, and J. A. Borchers, Phys. Rev. B **81**, 100405 (2010).
[8] B. J. Kirby, P. K. Greene, B. B. Maranville, J. E. Davies, and K. Liu, J. Appl. Phys. **117**, 063905 (2015).
[9] C. LeGraët, T. R. Charlton, M. McLaren, M. Loving, S. A. Morley, C. J. Kinane, R. M. D. Brydson, L. H. Lewis, S. Langridge, and C. H. Marrows, APL Mater. **3**, 041802 (2015).
[10] R. Skomski and D. J. Sellmyer, J. Appl. Phys. **87**, 4756 (2000).
[11] S. A. Ahern, M. J. C. Martin, and W. A. Sucksmith, Proc. R. Soc. A **248**, 145 (1958).
[12] A. F. Kravets, A. N. Timoshevskii, B. Z. Yanchitsky, M. A. Bergmann, J. Buhler, S. Andersson, and V. Korenivski, Phys. Rev. B **86**, 214413 (2012).
[13] A. Berger and E. E. Fullerton, J. Magn. Magn. Mater. **165**, 471 (1997).
[14] P. Riego and A. Berger, Phys. Rev. E **91**, 062141 (2015).
[15] K. Binder and P. C. Hohenberg, Phys. Rev. B **9**, 2194 (1974).
[16] "Quasi" because formally the order parameter is nonzero everywhere in an exchange coupled ferromagnetic system, if it is nonzero anywhere, even if it may be vanishingly small in large portions of the system.
[17] See Supplemental Material at http://link.aps.org/supplemental/10.1103/PhysRevLett.116.047203 for details regarding MFA simulations.
[18] See Supplemental Material at http://link.aps.org/supplemental/10.1103/PhysRevLett.116.047203 for details regarding PNR, including Refs. [19–21].
[19] B. J. Kirby, P. A. Kienzle, B. B. Maranville, N. F. Berk, J. Krycka, F. Heinrich, and C. F. Majkrzak, Curr. Opin. Colloid Interface Sci. **17**, 44 (2012).
[20] *ISO/IEC Guide 98-3-:2008/Suppl 1:2008, Propagation of distributions using a Monte Carlo method*, 1st ed. (International Organization for Standardization, Geneva, 2008).
[21] J. A. Vrugt, C. J. F. ter Braak, C. G. H. Diks, B. A. Robinson, J. M. Hyman, and D. Higdon, Int. J. Nonlinear Sci. Numer. Simul. **10**, 273 (2009).
[22] C. F. Majkrzak, K. V. O'Donovan, and N. F. Berk, in Neutron Scattering from Magnetic Materials, edited by T. Chatterji (Elsevier Science, New York, 2005).
[23] See Supplemental Material at http://link.aps.org/supplemental/10.1103/PhysRevLett.116.047203 for details of alternate PNR models, including Refs. [24,25].
[24] C. F. Majkrzak, Physica B (Amsterdam) **221B**, 342 (1996).
[25] I. S. Anderson, P. J. Brown, J. M. Carpenter, G. Lander, R. Pynn, J. M. Rowe, O. Schärpf, V. F. Sears, and B. T. M. Willis, *International Tables for Crystallography* (Wiley, Hoboken, NJ, 2006) Chap. 4.4, p. 430.
[26] Z.-P. Li, J. Eisenmenger, C. W. Miller, and I. K. Schuller, Phys. Rev. Lett. **96**, 137201 (2006).
[27] R. K. Dumas, Y. Fang, B. J. Kirby, C. Zha, V. Bonanni, J. Nogues, and J. Åkerman, Phys. Rev. B **84**, 054434 (2011).
[28] K. G. Sandeman, Scr. Mater. **67**, 566 (2012).
[29] C. W. Miller, D. D. Belyea, and B. J. Kirby, J. Vac. Sci. Technol. A **32**, 040802 (2014).